

Hot DQ White Dwarfs: Something Different

P. Dufour¹, G. Fontaine², James Liebert¹, G. D. Schmidt¹, N. Behara³

ABSTRACT

We present a detailed analysis of all the known Hot DQ white dwarfs in the Fourth Data Release of the Sloan Digital Sky Survey (SDSS) recently found to have carbon dominated atmospheres. Our spectroscopic and photometric analysis reveals that these objects all have effective temperatures between $\sim 18,000$ and $24,000$ K. The surface composition is found to be completely dominated by carbon, as revealed by the absence of $H\beta$ and He I $\lambda 4471$ lines (or determination of trace amount in a few cases). We find that the surface gravity of all objects but one seems to be "normal" and around $\log g = 8.0$ while one is likely near $\log g = 9.0$. The presence of a weak magnetic field is directly detected by spectropolarimetry in one object and is suspected in two others. We propose that these strange stars could be cooled down versions of the weird PG1159 star H1504+65 and form a new family of hydrogen and helium deficient objects following the post-AGB phase. Finally, we present the results of full nonadiabatic calculations dedicated specifically to each of the Hot DQ that show that only SDSS J142625.70+575218.4 is expected to exhibit luminosity variations. This result is in excellent agreement with recent observations by Montgomery et al. who find that J142625.70+575218.4 is the only pulsator among 6 Hot DQ white dwarfs surveyed in February 2008.

Subject headings: stars: abundances – stars: atmospheres – stars: evolution – white dwarfs

1. INTRODUCTION

White dwarfs represent the final stage of stellar evolution for the vast majority of stars that have exhausted the nuclear fuel available in their core (this is the fate of $\sim 97\%$ of

¹Steward Observatory, University of Arizona, 933 North Cherry Avenue, Tucson, AZ 85721; dufourpa@as.arizona.edu, liebert@as.arizona.edu, schmidt@as.arizona.edu

²Département de Physique, Université de Montréal, C.P. 6128, Succ. Centre-Ville, Montréal, Québec, Canada H3C 3J7; fontaine@astro.umontreal.ca

³CIFIST, GEPI, Observatoire Paris-Meudon, 92195, France; natalie.behara@obspm.fr

stars in our Galaxy). Standard stellar evolution theory predicts that a typical white dwarf is composed of a core that encompasses more than 99 % of the mass of the star, surrounded by a thin envelope of helium (and hydrogen) that has survived the nuclear burning and mass loss phase. The core, which is essentially the result of the fusion of light elements, has a composition that depends on the initial mass of the star. For very low mass stars that could not ignite helium, it is composed of helium. Stars at intermediate masses end up with cores composed of carbon and oxygen while the most massive stars produce oxygen-neon-magnesium (ONeMg) cores. The initial mass function and star formation history of the Galaxy are such that the majority of white dwarfs we observe in the solar neighborhood today have a core made of carbon and oxygen (the most massive white dwarfs are intrinsically rare while low mass stars producing helium core white dwarfs have nuclear lifetimes greater than the age of the disk of our Galaxy and are thus possible only from binary evolution or if the mass loss in the red giant phase is extremely large, Kalirai et al. 2007).

Direct observation of the core is unfortunately not possible since it is surrounded by a thin and opaque layer of helium (and hydrogen for $\sim 80\%$, see Iben 1984; Koester & Schönberner 1986; D’Antona & Mazzitelli 1987) that was left over in the the previous stage of stellar evolution. White dwarfs have thus traditionally been separated into two distinct families: those with a hydrogen rich surface composition, and those with a helium rich surface composition. The former are represented by the very well known DA white dwarfs while the latter family show more diversity in their spectral type. Indeed, although they all have a helium rich surface composition, they have been subdivided into several spectral types which reflect essentially their effective temperatures. The hottest ones ($T_{\text{eff}} > \sim 40,000$ K) that show He II lines are classified DO. At intermediate temperature ($\sim 12,000 - 40,000$ K), those showing exclusively He I lines are classified as DB. Stars too cool for the He I atoms to be sufficiently excited and show no features in their optical spectra are labeled DC. Finally, the cool helium dominated stars with traces of carbon (either molecular or atomic) in their optical spectra that are found between ~ 4000 K and $13,000$ K are classified as DQ white dwarfs.

Carbon is also observed in the spectra of the hot PG1159 stars, objects just entering or about to enter the white dwarf cooling phase. Their atmospheres show a mixture of helium, carbon and oxygen and little or no hydrogen (see Werner & Herwig 2006, and references therein). The most likely explanation for this unusual composition is that these stars have experienced the so-called "born again" scenario, i.e. a very late thermal pulse that has brought back the white dwarf onto the post-AGB phase for a second time early in its cooling phase (see Herwig et al. 1999, and references therein). As a result of this rather violent event, the star re-enters the white dwarf cooling phase but this time with a surface composition that is devoid of hydrogen. This process also mixes the remaining helium with elements from the envelope (mostly carbon and oxygen), producing the curious surface composition

observed in PG1159. Gravitational diffusion will eventually separate the helium from the heavier elements and PG1159 stars will thus turn into helium rich DO, then DB and finally DQ white dwarfs as the cooling continues.

The presence of carbon in cool DQ white dwarfs is now well explained by a model in which carbon diffusing upward from the core is brought to the photosphere by the deep helium convection zone (Pelletier et al. 1986). Detailed analysis of a large sample of 56 DQ stars by Dufour et al. (2005) showed that $\log (C/He)$ varies from about -7 at $T_{\text{eff}} \sim 6000$ K to -3 at $T_{\text{eff}} \sim 11,000$ K. The maximum contamination by carbon is predicted to be at $T_{\text{eff}} \sim 12,000$ K, i.e when the convection zone reaches its maximum. The only two stars close to this maximum that have been analyzed, G35-26 (Thejll et al. 1990) and G227-5 (Wegner & Koester 1985), have respectively T_{eff} of $12,500 \pm 1,500$ K and $12,500 \pm 500$ K and $\log (C/He) = -2$ and -2.5 . Parallax measurements (Dahn, private communication) have since shown that these two stars are massive white dwarfs ($\sim 1.1 M_{\odot}$). At these temperatures and abundances, the spectra show primarily C I lines and a hint of the He I $\lambda 4471$ line that is about to fade below visibility as the stars become too cool. While the cool range of the DQ distribution has been extensively analyzed thanks to the large sample from the SDSS (Dufour et al. 2005; Koester & Knist 2006), our knowledge of carbon abundances for hotter stars relies only on the two stars mentioned above and a few analyses of DB stars that show carbon only in the ultraviolet (Provencal et al. 2000; Dufour et al. 2002; Petitclerc et al. 2005; Desharnais et al. 2008).

The situation can now be improved dramatically thanks again to the discovery of several new hot DQ white dwarfs in SDSS (Liebert et al. 2003). Most of these stars have spectra similar to those of G35-26 and G227-5 and show essentially only C I lines (as opposed to molecular bands of C_2 for cooler stars). Surprisingly, some stars showed spectra that were dominated by C II lines. No detailed analysis could be performed at the time due to the lack of proper models for this type of stars. Estimates of effective temperatures based on pure helium models placed these stars well into the DB temperature range, although the exact atmospheric parameters were uncertain since analysis with pure helium models tends to overestimate the effective temperature (Provencal et al. 2002; Dufour et al. 2005). It was presumed that they were simply hotter versions of DQ stars like G35-26 and G227-5. Liebert et al. (2003) hypothesized that the dredge up of carbon for these special stars had happened earlier than usual because they were more massive and had a thinner outer helium layer, as the theoretical calculation of Kawai et al. (1988) show. It was believed that the increased continuum opacity resulting from the presence of the carbon was keeping us from detecting the strong helium lines that we usually see in DB spectra. According to the Liebert et al. (2003) scenario, the most massive DB stars simply dredged up carbon at hotter effective temperature, which made them to appear as hot DQ stars. The Beauchamp

(1995) and Voss et al. (2007) analyses of large samples of DB white dwarfs show that the DB mass distribution lacks the high mass component that is observed for DA white dwarfs. The scenario above was thus proposed as a natural explanation to the fact that the DB mass distribution morphology is fundamentally different from that of DA white dwarfs.

However, when we proceeded with the calculation of the appropriate models, we found that if helium was the dominant atmospheric constituent, it remained spectroscopically observable even when opacity due to a large quantity of carbon was accounted for. As a consequence, it seems that these stars have an atmosphere that is dominated by carbon with little or no trace of other elements. We could thus be directly witnessing the bare stellar CO core, or a carbon envelope around an ONeMg core, giving us a unique opportunity to test theories of stellar evolution. Note that standard dredge-up theory cannot explain this phenomenon since at the effective temperatures where these stars are found, the helium convection zone doesn't reach deep enough to bring a significant amount of carbon to the surface. Another explanation is thus required. According to the standard spectral classification defined in McCook & Sion (1999), white dwarfs that show carbon features, either atomic or molecular in any part of the electromagnetic spectrum are referred to as DQ. In order to avoid confusion with the cooler DQs, we will thus simply refer to stars that show mainly ionized carbon features as "Hot DQs", even though they are truly something different. The surprising discovery of these objects has been published recently in the form of a short letter (Dufour et al. 2007a). We now wish to present in more detail an up to date analysis of all the carbon dominated atmosphere white dwarfs that we have uncovered thus far as well as an in depth discussion of the possible origin and evolution of such objects.

In § 2, we describe the observations. Our theoretical framework including our model atmosphere and synthetic spectrum calculations are presented in § 3. The detailed analysis follows in § 4, and the results are interpreted and discussed in § 5. Our conclusions are summarized in § 6.

2. OBSERVATIONS

Our sample consists of white dwarf stars spectroscopically identified as "Hot DQ" in the SDSS Fourth Data Release white dwarf catalog of Eisenstein et al. (2006). Note that a fraction of the Hot DQs in this catalog are actually DQ white dwarfs in the 12,000-15,000 K temperature range that have helium-rich surface compositions ($\log(C/He) \sim -2$ to -3), and we do not include them in the present analysis (they will be analyzed in detail in Dufour et al., in preparation). Details concerning the observations can be found in Eisenstein et al. (2006) and reference therein. Our final sample consists of 9 Hot DQ stars with SDSS spec-

tra covering the 3800-9200 Å region at a resolution of ~ 3 Å FWHM. Also available are SDSS photometric observations on the *ugriz* system (Fukugita et al. 1996; Hogg et al. 2001; Smith et al. 2002; Ivezić et al. 2004). The spectra of a few of these stars have been previously shown in Liebert et al. (2003).

3. MODEL ATMOSPHERE AND SYNTHETIC SPECTRUM CALCULATIONS

The LTE model atmosphere code used for this analysis is similar to that described in Dufour et al. (2005, 2007b) and references therein for the study of cool DQ and DZ white dwarfs. It is based on a modified version of the code described at length in Bergeron et al. (1995), which is appropriate for pure hydrogen and pure helium atmospheric compositions, as well as mixed hydrogen and helium compositions, while energy transport by convection is treated within the mixing-length theory. One important modification is that metals and molecules are now included in the equation-of-state and opacity calculations (see Dufour 2007c, for details). The principal modification in the version used in this paper concerns the treatment of the continuum opacity of heavy elements. In our earlier version of the code, the bound-free and free-free opacities were taken from the Peach (1970) opacity tables. In the case of cool helium-rich white dwarf atmospheres (DQ, DZ and DC spectral type), the exact treatment of the metallic continuum opacity is not really important since the dominant source of opacity is the He^- free-free absorption. However, for hotter carbon-rich stars where the far-ultraviolet flux is far from negligible, it becomes important to include the best possible sources of opacity. Small variation in the absorption at short wavelengths can significantly modify the flux redistribution in these atmospheres as was shown by Behara & Jeffery (2005). Our models now include the latest photoionization cross-sections from the Opacity Project (1995, 1997) for CI-IV and OI-IV as well as the corresponding free-free absorption as described in detail in Behara & Jeffery (2006). Also, our earlier version of the code was dedicated to the analysis of cool white dwarfs in a regime where helium was spectroscopically invisible, and as a consequence, no effort was made to keep it up to date with the best He I line opacities (those of Beauchamp et al. 1997). The present version has thus been updated to include these He I line profiles. Since the charged carbon particles impose an electric micro-field at the location of the radiating atom, we also include a correction to the critical field strength and the plasma correlation parameter in the occupation probability formalism (Hummer & Mihalas 1988) as described in Werner & Wolff (1999).

The strongest C and O lines are included explicitly in both the model and synthetic spectrum calculations. These lines are selected by taking all lines contributing more than one

tenth of the continuum opacity at each optical depth. A test model calculated by including all the lines from our list was not found to yield any detectable difference on the emergent spectrum. The line absorption coefficient is calculated using a Voigt profile for every line at every depth point. Central wavelengths of the transitions, gf values, energy levels, and damping constants are extracted from the GFALL line list of R. L. Kurucz¹.

Two grids with different C/He and C/H abundance have been calculated. Our first grid covers a range from $T_{\text{eff}} = 16,000$ to $30,000$ K in steps of 2000 K, from $\log g = 7.5$ to 9.0 in steps of 0.5 dex, and from $\log (\text{C/He}) = +3.0$ to 0.0 in steps of 1.0 dex. Our second grid covers the same parameter space except that it is $\log (\text{C/H})$ varying from $+3.0$ to 0.0 in steps of 1.0 dex. Finally, additional models with various abundances of oxygen have been calculated to explore the sensitivity of our results to this unknown parameter. Illustrative spectra from our grid are displayed in Figure 1 for various values of the effective temperature, gravity, hydrogen and helium abundances.

4. DETAILED ANALYSIS

4.1. Fitting Technique

The effective temperatures of the stars can be determined from either the photometric energy distributions or from fits to the carbon lines. In both cases, the fitting procedure relies on the nonlinear least-squares method of Levenberg-Marquardt (Press et al. 1992).

In the first case, we fit the *ugriz* colors with both T_{eff} and the solid angle $\pi(R/D)^2$, which relates the flux at the surface of the star to that received at Earth (R is the radius of the star and D its distance from Earth), as free parameters. This is done for a fixed value of $\log g$ and $\log (\text{C/He})$ or $\log (\text{C/H})$ (we will explore the effect of the former below while the latter are constrained/determined from the absence/presence of spectroscopic features). Corrections of the photometric measurements to account for the extinction from the interstellar medium are obtained from the reddening maps of Schlegel et al. (1998). We experimented with various fractions of the absorption in the line of sight to assess the effect of this unknown parameter on our atmospheric parameter determinations (see below). Finally, we compare the observed spectra with the synthetic spectra interpolated at the solution obtained from the photometric fit.

In the second case, we do the inverse. That is we first fit the carbon lines from the

¹see <http://kurucz.harvard.edu/LINELISTS.html>

spectroscopic data to obtain the effective temperature (with the solid angle and the slope, to account for the unknown amounts of reddening and spectrophotometric errors, left as free parameters) and then fit the photometric data with T_{eff} fixed to that value to obtain the solid angle (this gives the photometric distance, see Table 1) and assess the quality of the solution. Again, this is done for various fixed values of $\log g$ and $\log (\text{C}/\text{He})$ or $\log (\text{C}/\text{H})$.

4.2. Hydrogen and Helium Abundances

With the possible exception of one star, none of the Hot DQ stars analyzed in this paper show the presence of helium (He I λ 4471). Therefore, only upper limits can be set from the spectroscopic observations. These limits depend sensitively on the range of effective temperature considered. We roughly estimate these limits by inspecting our grid of synthetic spectra. We estimate, for the typical signal-to-noise ratio of the SDSS observations, that at $\log g = 8$, the threshold for the detection of helium as a function of effective temperature is at $\log (\text{C}/\text{He}) \sim 0.7$ for $T_{\text{eff}} = 18,000$ K, ~ 1.6 for $T_{\text{eff}} = 22,000$ K and ~ 1.8 for $T_{\text{eff}} = 26,000$ K. At higher gravity, the $\lambda 4471$ line becomes very broad and much more helium can be present without being observable. For example, at $\log g = 9$, the limits are $\log (\text{C}/\text{He}) \sim 0.0$ for $T_{\text{eff}} = 18,000$ K while at $T_{\text{eff}} = 22,000$ K the limit is ~ 1.0 .

The limits on the amount of hydrogen are more difficult to assess, since the H α line is contaminated by strong carbon features. The H β line is thus used to set the limit of visibility of hydrogen since it is free of contamination for most of the range of effective temperature we are exploring. We find that H β is spectroscopically observable for $\log (\text{C}/\text{H}) \sim 2.7$ for T_{eff} below $\sim 23,000$ K. At higher effective temperature, a carbon line starts to become strong at the position of H β and no limit can be obtained with complete certainty.

We note that the influence of small, spectroscopically invisible amounts of hydrogen or helium do not affect significantly the effective temperature determination (except for the coolest star, see below) and that fits without hydrogen or helium are practically identical to those with H and He set at the limits of visibility.

4.3. Atmospheric Parameter Determinations

SDSS J000555.90–100213.3 : The spectrum of this star shows an obvious sign of magnetic line splitting. The ~ 4270 Å line seems to be split into three components approximately 25 Å apart, corresponding to a mean surface field strength of $B_S \approx 1.47$ MG (see eq. 3 in Dufour et al. 2006, where an effective Landé factor equal to unity is assumed). Circular

spectropolarimetry obtained with the spectropolarimeter SPOL (Schmidt et al. 1992) on the 2.3 m Bok reflector at Kitt Peak confirms the presence of a magnetic field on *SDSS J000555.90–100213.3*. These data were acquired on 2007 Oct. 17 and Dec. 14 using a single order of a low resolution grating ($\Delta\lambda \sim 17 \text{ \AA}$) to cover the region 4000–8000 \AA . Polarimetric sequences each totaling 4800 s were obtained both nights, and because the results were indistinguishable within the statistical noise, the average is displayed in Figure 2. Clear polarization reversals are seen around the prominent C II lines at $\lambda\lambda 4267, 4370$, near $\lambda 4860$, and, with somewhat less significance, at the broad, shallow $\lambda 6578, 6583$ C II feature. The $\lambda 4860$ polarimetric feature is real, as it is present in both data sets, despite the fact that a strong absorption line is not observed here. However, inspection of the flux spectra from the SDSS as well as from our data reveal that the region is clearly affected by a number of weaker lines. The longitudinal magnetic field is difficult to estimate from the data because the Zeeman splitting is actually somewhat less than the separation between the two components that comprise the $\lambda 4300$ feature, and the $\lambda 6580$ line is both shallow and noisy. However, simulations of the blue feature using reasonable intrinsic line profiles suggest that a mean longitudinal value $B_e \sim 400 - 800 \text{ kG}$ is appropriate for the data. This is consistent with the estimate of mean surface field $B_S \approx 1.47 \text{ MG}$ based on the observed splitting of the line core into three Zeeman components. The presence of the magnetic field seems to have destroyed all the carbon features that are strongly seen in most other objects of our sample. As a consequence, we cannot estimate the effective temperature by fitting the lines and thus use the photometric data. For the same reason, we cannot constrain or estimate the surface gravity for this star. We thus assume $\log g = 8.0$. Our fit of the energy distribution yields $T_{\text{eff}} = 17,400 \text{ K}$ if no reddening correction is applied and $T_{\text{eff}} = 19,420 \text{ K}$ if we assume the full correction from the Schlegel et al. (1998) maps. The corresponding fit to the solid angle places this star at a distance of $\sim 250 \text{ pc}$. A fair fraction of the extinction on that line of sight should thus be applied so we believe that the hottest solution is probably more realistic. This is this solution that we show in Figure 3 and Table 1.

SDSS J010647.92+151327.8 : The extinction in the line of sight to this star is particularly high and as a result, the photometric fits with and without correction for the extinction are very different (T_{eff} of respectively 17,900 and 22,900 K). The synthetic spectra interpolated to the photometric solution without correction for the extinction is clearly at odds with the observed spectra while the hotter solution looks better even though it suffers from obvious flaws. First, the 4270 line is predicted to be too strong and the features near 4100–4200 \AA are also poorly reproduced. There might also be a small amount of hydrogen as suggested by the feature near $H\beta$. If we believe the small absorption near $\lambda 4471$, this object might be the only one in our sample showing a trace of helium. We can approximately reproduce the $\lambda 4471$ feature if we allow $\log (\text{C/He}) \sim 1.0$. Fits with this abundance yield $T_{\text{eff}} = 23,430 \text{ K}$,

making this star the hottest of our sample. It is possible that the lines are also affected by the presence of a weak magnetic field, but polarization measurements are needed to confirm this hypothesis. We thus do not attempt to fit the lines individually and only give our $\log g = 8.0$, $\log (\text{C}/\text{He}) = 1.0$ photometric fit with full correction for extinction in Figure 3 and Table 1.

SDSS J023637.42–073429.5 : Our $\log g = 8.0$ photometric fits with and without correction for the extinction give respectively $T_{\text{eff}} = 22,960$ and $20,780$ K. Both synthetic spectra interpolated at these solutions compare reasonably well with the observations considering the signal-to-noise ratio of the spectrum. It is reassuring that if we use only the spectra in our minimization technique, we get an effective temperature that is intermediate at $T_{\text{eff}} = 21,100$ K. As for the surface gravity, a value as high as $\log g = 9.0$ is clearly ruled out, since the resulting line profiles would be far too broad to be compatible with the observation. However, a value of $\log g = 8.5$ cannot be dismissed but a higher signal-to-noise ratio observation will be needed to better constrain this parameter.

SDSS J115305.54+005646.2 : Our $\log g = 8.0$ photometric fits with and without correction for the extinction give respectively $T_{\text{eff}} = 21,400$ and $20,160$ K. Inspecting the resulting synthetic spectra, we find that the hotter solution looks is a slightly better match. The solution by fitting the lines confirms that result, since it yields $T_{\text{eff}} = 21,650$ K. Although the overall appearance of the fit looks very good (see Figure 3), several discrepancies catch our attention. In particular, we notice that the strengths of the four weaker lines that follow the strong $\lambda 4270$ are not well reproduced by our model. The first is barely seen in our synthetic spectra, while the second is too strong. The third and fourth have about the right strength, although the fit is far from perfect. We note also that the strong feature near ~ 5130 Å is poorly reproduced. Finally, the line near ~ 4960 Å is not predicted at all by our models for this effective temperature (it starts to appear only at about $26,000$ K, see Figure 1). In fact, if we look carefully at Figure 1, we notice that all the above mentioned lines have the right strength only at a much higher effective temperature than what we have determined here. It seems as if that these few lines, and only these few ones, required a higher effective temperature. We will discuss in more detail in the next section possible explanations for these discrepancies. As for surface gravity, as it is the case for all the objects in our sample, the quality of the data at hand (as well as the problem with the strengths of some lines noted above) does not allow us to precisely determine this parameter. However, the value of $\log g$ is probably not too far from 8.0 since for fits with $\log g$ fixed at 8.5 , we already find that the lines are broader than observed.

SDSS J133710.19–002643.7 : This star is very similar to *SDSS J023637.42–073429.5*, except for the clear presence of hydrogen as revealed by the $\text{H}\beta$ line. Our $\log g = 8.0$ pho-

tometric fits with and without correction for the extinction give respectively $T_{\text{eff}} = 22,550$ and $20,770$ K. Both synthetic spectra interpolated at these solutions compare reasonably well with the observation, considering the signal-to-noise ratio of the spectrum. Again, it is reassuring that if we use only the spectra in our minimization technique, we get an effective temperature that is intermediate at $T_{\text{eff}} = 21,670$ K. The value $\log(C/H)$ we get for that temperature is 1.67. The surface gravity seems to be near $\log g = 8.0$ and perhaps even less. A surface gravity as high as $\log g = 8.5$ is completely ruled out, since that would produce lines that are too broad to be compatible with the observation. We note that again, we observe some discrepancies in the line strength of the four lines long-ward of the ~ 4270 line and the line near ~ 4960 .

SDSS J142625.70+575218.4 : The spectrum of this star doesn't show as many carbon lines as we see in most other objects. There is a strong feature near ~ 4270 Å and hints of absorption for a few more lines. Our $\log g = 8$ fit indicates that this star is one of the coolest of the sample with an effective temperature of about 17,000-17,500 K. However, optical synthetic spectra with such parameters are predicted to show many strong carbon features, in particular the group of lines long-ward of ~ 4270 Å that are not observed in the SDSS spectrum. Inspection of Figure 1 indicates that synthetic spectra having similar characteristics to *SDSS J142625.70+575218.4* exist for a higher T_{eff} and $\log g$. We believe we can thus reject a low surface gravity solution and that $\log g$ near 9.0 is more likely. If we fix $\log g$ at 9.0, we get a good fit of the energy distribution at $T_{\text{eff}} = 17,800$ K but the lines long-ward of ~ 4270 Å still remain too strong. If we use only the spectrum in our minimization procedure, we achieve a much better fit at $T_{\text{eff}} = 20,500$ but then the u, r and z band fluxes are poorly reproduced. At high gravity and low effective temperature, much more helium can be hidden without being spectroscopically observable. In this particular case, the presence of helium does affect slightly our atmospheric parameter determination. If we assume $\log g = 9.0$ and $\log(C/He) = 0.0$, we obtain a very acceptable fit for the spectrum at $T_{\text{eff}} = 19,830$ K and only the u band is slightly over predicted. This solution (this is the one we present in Figure 3 and Table 1) also predicts a tiny depression from the He I $\lambda 4471$ line that is compatible with the observations (the spectrum seems to show a possible glitch at the right position but better signal-to-noise ratio observations are required to confirm the presence of helium). It is also possible that the surface gravity exceeds 9.0 and that a better solution exists outside the parameter space of our grid. Finally, we notice that our solution does not predict correctly the strength of the ~ 4620 Å line, suggesting perhaps that the effective temperature might actually be a little higher.

SDSS J161531.71+454322.4 : This star is one of the few that shows the presence of a $H\beta$ line. Our photometric fits with and without correction for extinction give an effective temperature of, respectively, 18,300 and 17,600 K. However, these solutions predict an optical spectrum

that is clearly at odds with the observation. The strengths of the observed lines seem to indicate that the effective temperature is much higher. If we use only the spectrum in our minimization procedure, we get a much better fit with $T_{\text{eff}} = 20,940$ K and $\log(C/H) = 1.74$. The price to pay with this solution is that the u band flux is predicted to be much stronger than observed. Higher surface gravity solutions are ruled out as even for $\log g = 8.5$, the predicted line profiles are too broad.

SDSS J220029.09–074121.5 : Our $\log g = 8.0$ photometric fits with and without correction for the extinction give respectively $T_{\text{eff}} = 21,200$ and $18,500$ K. From the inspection of the predicted optical spectra at these solutions, we can easily reject the coolest of the two, as the line strengths are then poorly reproduced. If we fit only the lines, we get $21,240$ K and this is thus the solution that we present in Figure 3 and Table 1. We note that the observed ~ 4270 Å line is much broader than predicted, indicating perhaps that the surface gravity is higher than $\log g = 8.0$. However, if we try to fit this star with a higher gravity, we get a better fit to the ~ 4270 Å line but then all the other lines are too broad. One attractive possibility is that the line profiles for this star are affected by the presence of a weak magnetic field but the lines are not separated enough to be individually identified. Polarimetric measurement should easily confirm the validity of this hypothesis.

SDSS J234843.30–094245.2 : The $\log g = 8.0$ photometric solutions with and without correction for extinction give respectively $T_{\text{eff}} = 17,600$ and $16,000$ K. At these temperatures, the predicted optical spectra are clearly at odds with the observations. A much better fit at $T_{\text{eff}} = 21,550$ K can be obtained by using only the line profiles in our minimization procedure. However, the corresponding energy distribution with this solution is poorly reproduced. We have no explanation for such a discrepancy. A higher surface gravity is again ruled out, as the predicted line profiles would be too broad. We note again that we observe some discrepancies in the line strength of the four lines long-ward of the ~ 4270 line, the line near ~ 4960 and another near ~ 5260 Å .

4.4. Source of Uncertainties

4.4.1. Flux in the ultraviolet

At the effective temperatures where the carbon dominated atmosphere white dwarfs are found, a large fraction of the light is emitted in the UV portion of the electromagnetic spectrum. Figure 4 shows two synthetic spectra at $T_{\text{eff}} = 22,000$ K for pure helium (red) and a pure carbon atmosphere (blue). The most striking characteristic is the strength and number of all the carbon features in the UV part of the spectra in the pure carbon model

while the DB model is practically featureless in the same region. These absorptions in the UV have a huge impact on the energy distribution. This can easily be appreciated by remembering that the total energy emitted, $\int H_\nu d\nu$, is by definition, for a given T_{eff} , the same for both models ($= \sigma T_{\text{eff}}^4/4\pi$). All the flux below $\sim 1500 \text{ \AA}$ that is absorbed in the pure carbon model, compared to the DB model, is redistributed at longer wavelengths. It is thus important to include as accurately as possible all sources of opacity in the model calculation, as errors in our treatment of the absorption in the UV might have significant impact on the thermodynamic stratification and the overall energy distribution. These errors can be of multiple origins. The line list we use can be incomplete, values of $\log gf$ for some lines might be wrong by unknown factors, unexpected absorption from other elements might be present, or the broadening theory we use might be incorrect (see below for more on that issue). It is thus quite possible that the above mentioned discrepancies observed for many lines in the optical might be related to such errors (alternatively, the few lines that have $\log gf$ errors in our list might just stand out).

Therefore, until UV observations are obtained to assess the quality of our modeling of that part of the spectrum, our atmospheric parameter determinations remain uncertain. It is probable that, as we learn more on these various aspects, future generation of models will have different thermodynamic stratification which could yield slightly different atmospheric parameters. It is difficult to quantify this for the moment, since no UV observations are yet available, but given the inconsistencies enumerated above (i.e. the few lines that are poorly reproduced), it is possible that our effective temperature determinations could perhaps be wrong by as much as 2000 K, a larger value than what is reflected in the formal statistical uncertainties presented in Table 1.

On the other hand, due to the richness of the UV part of the spectra, these stars give us a unique opportunity to test the accuracy of the theoretical atomic data, opacity sources and broadening theory for the carbon atom since we are observing carbon in physical conditions and abundances never seen previously. Detailed comparison of state of the art models with future UV observations should allow us to better assess the quality of our modeling and reduce significantly the uncertainties on our derived atmospheric parameters.

4.4.2. *Influence of Oxygen*

Since oxygen is also expected to be present in large proportion, along with carbon, in the cores of white dwarf stars, we discuss in this section how it could influence our results if present in the atmosphere. In figure 5, we show synthetic spectra of $\log g = 8$, $T_{\text{eff}} = 22,000 \text{ K}$ atmosphere models with a pure surface composition of hydrogen, helium, carbon

and oxygen. We first notice that for a pure oxygen model, the optical spectrum is not as rich in spectral features as those made with lighter elements. With the exception of a few strong lines, most of these features would not even be identifiable in a spectrum as noisy as our SDSS Hot DQ stars. Inspection the 9 Hot DQ spectra did not reveal any evidence of an oxygen feature at the position of the strong oxygen lines seen in Figure 5. Models assuming a surface composition of 50% C and 50% O are also very similar to those of 100% C, except that the strongest oxygen lines can be noticed and that the carbon lines appear a little bit broader. However, since we do not observe these oxygen lines in any of our spectra, the oxygen abundance has to be at least close to an order of magnitude inferior to that of carbon. A more precise limit will require the analysis of higher signal-to-noise ratio observations, but since the C/O ratios are certainly much higher than one, this practically guarantees that the atmospheric parameters derived in this study should not significantly be altered by the presence of an unknown but small amount of oxygen.

4.4.3. *Stark Broadening*

The dominant source of broadening in the conditions encountered in these type of stars is Stark broadening. In this first generation of carbon atmosphere models, we made use of the so-called "scaled classical approximation" (Kurucz & Avrett 1981; Hubeny 1988). This approximation assumes Γ_S/N_e to be a constant. How realistic this approximation is under the atmospheric conditions met here remains to be tested. Uncertainties associated with the precision of the treatment of the line broadening of C II could thus prove to be a large source of error in our model calculations and surface gravity estimations. As discussed above, errors in the absorption coefficient can have a particularly strong effect in the UV part of the spectrum, not to mention the line profiles in the optical. We thus believe we should remain very cautious in our interpretation of the limits/determinations of the surface gravity as derived from the line profiles. We are currently working on incorporating the best Stark broadening theory available for C II lines in our model calculations and the results will be presented in due time.

5. DISCUSSION

5.1. Spectral Evolution Scenario

In this section, we present what we believe is a most likely scenario for the formation and evolution of carbon atmosphere white dwarfs. The main line of our argument has been

briefly discussed in Dufour et al. (2007a) and Dufour et al. (2007d).

The origin of hydrogen deficient stars is generally believed to be explained by a late helium-shell flash where a post-AGB star (or white dwarf) re-ignites helium-shell burning. This brings the star back onto the AGB phase (the "born again" scenario) and the associated envelope mixing and mass loss eliminate the remaining hydrogen. As a result, the surface composition of these objects will be a mix of helium, carbon and oxygen. PG1159 and non-DA (helium-rich) stars are probably descendants of objects that have experienced this late flash. It is thus certainly not too far-fetched to imagine that a particularly violent late thermal pulse could also explain the origin of stars that are both hydrogen *and* helium deficient. The hottest PG1159 star H1504+65 ($T_{\text{eff}} \sim 175,000$ K) might actually owe its origin to such a scenario. Its surface composition is nothing short of amazing with a mass fraction of C $\sim 48\%$, O $\sim 48\%$, Mg $\sim 2\%$ and Ne $\sim 2\%$ and until the recent discovery of the Hot DQ white dwarfs, H1504+65 was the only known object to not show traces of either hydrogen or helium (Werner 1991; Werner & Wolff 1999; Werner et al. 2004). It is thus very tempting to draw an evolutionary link between H1504+65 and the cooler carbon dominated atmosphere white dwarfs.

As a star like H1504+65 cools, it is expected that gravitational diffusion will separate carbon from oxygen so that the atmosphere should rapidly appear carbon dominated. One flaw to this simple scenario is that we would expect to find carbon dominated atmospheres all along the cooling sequence, not only in a narrow strip centered around $\sim 20,000$ K. However, a careful search through the SDSS archive didn't reveal any new carbon dominated white dwarfs with an effective temperature higher than those presented in this paper (we looked at all the DR6 spectra with $u - g < -0.2$ and $g - r < -0.3$). Thus, even though our sample is small, it is certainly significant that *all* objects are found in a narrow effective temperature strip and *none* at higher or lower temperature. Any proposed scenario must be able to explain this extraordinary fact.

On the other hand, we do not believe that this necessarily mean that there is no possible relationship between stars like H1504+65 and the Hot DQs. Even though helium is not detected in the atmosphere of H1504+65, it doesn't mean that none is present since this star is so hot that a small amount of helium could be present but completely ionized, preventing its detection from spectral analysis (Nousek et al. 1986). Hence, the small residual amount of helium possibly existing in the envelope of H1504+65 should eventually diffuse upward to form a thin layer above a carbon-enriched and oxygen-depleted mantle. Since the total mass of an atmosphere is tiny ($\sim 10^{-14} - 10^{-15} M_{\odot}$), there should ultimately be enough accumulated helium to form a full atmosphere and the descendant of H1504+65-like stars should then "disguise" themselves as He-atmosphere white dwarfs following the PG1159

evolutionary phase. We believe that these helium-rich stars could then cool normally as DO/DB stars until a convection zone develops in the carbon-enriched mantle due to the recombination of that element. At that point in time, the subphotospheric carbon convection zone becomes active enough to be able to dilute from below the very thin overlying radiative He layer and the star undergoes a dramatic spectral change, transforming itself from a He-dominated atmosphere white dwarf to a carbon-dominated atmosphere star. Since the mass in the carbon convection zone is orders of magnitude larger than the mass of the He layer, helium would become spectroscopically invisible. The exact value at which this dilution take place is not known due to a current lack of proper modelling, but it is conjectured that it should be around 24,000 K. SDSS J010647.92+151327.8, the hottest and the only star clearly showing helium in our sample could perhaps be a rare star caught in the act of converting from a DB to a Hot DQ.

In addition, the carbon dominated atmosphere phase in the evolution of such a star must be short-lived as no carbon dominated cases are found for effective temperatures lower than $\sim 18,000$ K. Such stars, if they existed, would not only be easily recognizable from their spectra (the atomic or molecular features would be extremely strong, see Fig. 6), but should also be more numerous since the cooling times are much longer as we approach the low end of the cooling sequence (in other word, stars tend to accumulate at low effective temperature while they pass rapidly through the hotter phase). The fact that we haven't uncovered them probably means that helium must ultimately reappear at the surface in enough quantity to form again a helium-rich atmosphere (high signal-to-noise ratio observation revealing the presence of helium in one of the coolest stars in our sample, SDSS J142625.70+575218.4, would certainly strengthen this scenario). Since the total amount of helium present in such stars is probably much smaller than what is expected from "normal" stellar evolution, they would have thin helium layers.

In fact, we do know a group of stars that just may have such a characteristic: the DQ white dwarfs belonging to the "second sequence" (Dufour et al. 2005; Koester & Knist 2006). Indeed, while the majority of DQ stars form a clear sequence in a $\log(C/He)$ vs. T_{eff} diagram (see Fig. 12 of Dufour et al. 2005), several stars were found to have carbon abundances that lie about 1 dex above the more populated "main" sequence (this was also confirmed with an even larger sample by Koester & Knist 2006). The sequence where the bulk of the DQ stars are found is naturally explained by the standard dredge-up model and it is in agreement with the expectation that the envelopes of post-AGB stars should have $\log q(\text{He}) \equiv \log M_{\text{He}}/M_{\star}$ around -2 or -3. Only one star located on the second sequence has a mass determination as estimated from the parallax measurement. Since it was much more massive than all the others ($1.05 M_{\odot}$ vs $\langle M \rangle = 0.59 M_{\odot}$ for the others), it was hypothesized that maybe stars on the second sequence were just more massive as a group and that this could explain the higher

than usual carbon abundance. However, detailed evolutionary calculations by Brassard et al. (2007, see their Figure 1) showed that massive white dwarf evolution cannot account for the high abundances in the coolest DQ white dwarfs and that thin helium envelope model could be a better explanation. Could these special DQ white dwarfs be cooled down versions of the hot DQs ? We believe this is a very plausible possibility that deserves more scrutiny.

To summarize, we propose that the Hot DQs represent a short phase in what appears to be a new channel in stellar evolution. Hence, in addition to the general evolutionary sequence PG1159-DO-DB-DQ, there could be another one involving H1504+65-like stars and the hot DQ white dwarfs. This is schematically shown in Figure 7. Star like H1504+65, showing initially a mixed C and O atmosphere, would show a carbon dominated atmosphere after an intermediate phase in which it would have been observed as a DO or DB white dwarf. With further cooling, the small amount of helium believed to be diluted in the massive carbon envelope would rise again to the surface and the star then would appear as a highly polluted DQ white dwarf. Evolutionary calculations are awaited to quantitatively test the various aspects of this scenario.

5.2. Other scenarios

Are there other scenarios that could also explain the existence of hydrogen and helium deficient objects ? One could argue that the merging of two CO white dwarfs with a total mass less than $1.4 M_{\odot}$ could produce such a thing. Or perhaps the presence of a close companion may help to strip away the superficial layers of a white dwarf, exposing the core. Imaginative theorists may also succeed in finding several other ways to explain the weird surface composition of the Hot DQ. However, there is one factor that we find very difficult to reconcile with the above mentioned hypotheses (or any other kind of scenario for that matter): why do they all have effective temperatures between 18,000 and 23,000 K ? For all alternative scenarios we could conceive of, the probability of finding a star outside this temperature range is always greater than finding one inside. Unless future surveys actually succeed in finding several new carbon-dominated atmosphere white dwarfs outside this temperature range, our proposed scenario involving episodes of diffusion and convective mixing along the cooling sequence remains, in our view, the most likely.

The exact evolutionary history of the Hot DQs and H1504+65, related or not, is still unknown. As was perhaps the case with H1504+65, it may also be possible for the mass loss phases of white dwarfs of ordinary mass reaching C-O cores to lose most or all of their helium layers, exposing the naked core of a former AGB star. Alternatively, a series of five papers (García-Berro & Iben 1994; Ritossa et al. 1996; García-Berro et al. 1997; Iben et al.

1997; Ritossa et al. 1999) calculated the evolution of 9, 10, 10.5 and 11 solar masses stars. Only the last case made it to the Fe peak and would explode as a supernova. The models in the 9-10.5 M_{\odot} range produce massive cores at the end of the helium-burning phase, and rise in temperature enough to ignite carbon in a series of weak flashes, burning the carbon core stably, and producing ONeMg cores of $> 1.2 M_{\odot}$. During the second asymptotic giant branch phase, there are good chances that almost all of the helium (as well as all of the hydrogen) would be lost. This would leave a carbon-oxygen envelope/atmosphere that could explain the origin of carbon-dominated atmospheres white dwarfs, if the white dwarfs are massive. The following spectral and chemical evolution of the surface could then have followed a similar path as described above in order to be found only between 18,000 and 23,000 K.

At face value, our $\log g$ estimations generally favor a stronger-than-usual mass loss from a C-O core star, as for only one star (SDSS J142625.70+575218.4) is there a good case for $\log g$ around 9. For the others, $\log g$ near 8 gives the best fits, while $\log g$ as high as 8.5 can be ruled out for most. It is possible that both mechanisms work, and that SDSS J142625.70+575218.4 indeed came from a progenitor higher than 8 M_{\odot} while the others have a different origin. It is thus important to firmly establish whether stars initially as massive as 9-10.5 M_{\odot} can produce white dwarfs with the properties that we observe. However, given the many uncertainties cited above, in particular the Stark broadening of C II lines and the UV flux level, our surface gravity determinations are only preliminary and we will refrain from drawing any definitive conclusions at this point.

5.3. Pulsation Survey

One additional interesting aspect of Hot DQ white dwarfs that has not escaped our attention is that past models of carbon-atmosphere white dwarfs in the range of effective temperature where the real ones are found (see Fontaine & van Horn 1976) are characterized by an important outer superficial convection zone, very similar to that found in the pulsating DB (centered around $T_{\text{eff}} \simeq 25,000$ K) or in the pulsating DA stars (found around $T_{\text{eff}} \simeq 12,000$ K). Hence, it follows that carbon-atmosphere white dwarfs could also excite pulsation modes through the same partial ionization/convective driving phenomenon that is at work in these two distinct families of pulsating white dwarfs.

With this background in mind, Fontaine et al. (2008) recently investigated the asteroseismological potential of Hot DQ's with the help of full nonadiabatic calculations. They searched for possible instability regions in parameter space defined by the effective temperature, the surface gravity, the C/He ratio, and the convective efficiency. Given the right location in parameter space, they found that some Hot DQ stars should show pulsational

instabilities against gravity modes. In some cases, dipole ($\ell = 1$) g -modes with periods in the range 100–700 s can be excited. The blue edge of the predicted instability strip is hotter for higher gravity objects, while increasing the C/He ratio in the atmosphere/envelope tends to extinguish pulsational driving.

In parallel to this effort, an independent observational search for luminosity variations in the current sample of Hot DQ white dwarfs was initiated by Montgomery et al. (2008) at the McDonald Observatory. In February 2008, they monitored the six accessible stars in the current sample (SDSS J010647.92+151327.8 through SDSS J161531.71+454322.4 in Table 1) and found overwhelming evidence for variations in the light curve of SDSS J142625.70+575218.4 (see their Fig. 2), thus uncovering the prototype of a new class of pulsating star. At the same type, no variations with amplitudes above the detection threshold were observed in the five other targets. The discovery that SDSS J142625.70+575218.4 is a pulsating star is an extremely significant finding as it opens the door to the application of the tools of asteroseismology to the further study of Hot DQ white dwarfs. In essence, a new chapter in asteroseismology has started with that discovery.

We take advantage here of our preliminary determinations of the atmospheric properties of Hot DQ stars summarized in Table 1 to follow up on the exciting discovery of Montgomery et al. (2008). We compute, for each of the nine objects, a dedicated full stellar model using our estimates of T_{eff} , $\log g$, and the C/He ratio. We assume a structure with an envelope specified by a uniform chemical composition defined by that C/He ratio, on top of a C/O core in equal proportions by mass. For the purposes of the driving/damping process, only the chemical composition of the envelope is of relevance (see Fontaine et al. 2008). We finally vary, for each target, the assumed convective efficiency in the model from the so-called ML2 version of the mixing-length theory, to the more efficient ML3 flavor. Hence, for each star in Table 1, we constructed two stellar models specified by the given values of T_{eff} , $\log g$, and C/He, one with ML2 convection and the other with ML3 convection. For those objects with no tabulated value of C/He, we used the visibility limits quoted in Subsection 4.2; this maximizes the possible He content and therefore the possibility of pulsational driving.

We analyzed each equilibrium model using a full nonadiabatic approach. We find that eight stars out of nine – those with values of $\log g = 8.0$ in Table 1 – are not expected to pulsate. This is mostly due to the fact that their atmospheres/envelopes appear too carbon-rich to be able to drive pulsations at their estimated values of T_{eff} . Their effective temperatures are indeed significantly higher, even taking into account the uncertainties given in Table 1, than the expected theoretical blue edges for a surface gravity $\log g = 8.0$ and the various C/He ratios involved. On the other hand, we find that a model of SDSS J142625.70+575218.4 with $T_{\text{eff}} = 19,830$ K, $\log g = 9.0$, C/He = 1, and ML3 convection is

able to excite dipole g -modes in the interval 163.9–293.8 s. While this falls somewhat short of the period of 417.7 s found for the dominant periodicity in SDSS J142625.70+575218.4 (Montgomery et al. 2008), this should not be cause for concern at this stage because our estimations of the atmospheric parameters of that faint pulsator need to be improved as indicated above. We plan to actively pursue that endeavor with the MMT. For the time being, we conclude that the expectations that we can infer from nonadiabatic pulsation theory fall nicely in line with our determinations of the atmospheric parameters of Hot DQ white dwarfs in conjunction with the interesting results of Montgomery et al. (2008).

6. SUMMARY AND CONCLUSIONS

We presented a detailed spectroscopic and photometric analysis of the 9 Hot DQ white dwarfs with carbon dominated atmospheres that have been discovered in SDSS DR4. Strong upper limits on the abundance of hydrogen and helium are obtained from the absence of $H\beta$ and $He\ 1\lambda 4471$, while in a few cases, small amounts of hydrogen or helium are found in a carbon dominated atmosphere. The presence of a magnetic field is detected in one star, while the spectra from two others suggest the possibility of the presence of a weak field as well. Our analysis also reveals that these stars are all situated in a narrow range of effective temperature ($\sim 18,000$ – $24,000$ K) and that all, except one, seem to have normal surface gravity (around $\log g = 8.0$). Admittedly, the precision of that result is very uncertain due in part to the low signal-to-noise ratio of the data. Additionally, this first generation of carbon atmosphere models must be considered preliminary, as many factors might influence our results (opacity sources in the UV, broadening theory etc.). We retain two main hypothesis for the origin of these stars i) They might be the results of C-O core white dwarfs that have experienced an unusually high mass loss at the end of the AGB phase or ii) be the progeny of massive stars that had carbon burning and produced O-Mg-Ne cores white dwarfs. If the latter is the case, the hot DQ stars may ultimately help to better define the limiting mass at which massive stars explode as a type II supernova as well as the birth rate of neutron stars.

Future work on these objects will be dedicated to the analysis of higher signal-to-noise ratio observations. Follow up spectroscopic observations with the Mount Hopkins 6.5m MMT telescope and the Mount Fowlkes Hobby Eberly Telescope are underway and will be present in due time. Our next generation of model atmospheres for carbon dominated compositions should include the latest Stark broadening theory of C II lines as well as any updates on sources of opacity that are judged necessary. We also hope to obtain time for near-UV and far-UV observations with the Hubble Space Telescope (HST) using the Cosmic Origin Spectrograph (COS), after the scheduled repair mission, to assess the quality of our modeling

of the UV part of the spectrum. Finally, now that we know how to easily recognize these stars, we are paying special attention to SDSS data releases so that the number of objects in this new interesting spectral class is expected to increase in a near future.

We wish to thank D. Eisenstein for very useful discussions concerning the SDSS data and the DR4 white dwarfs catalog and P. Smith for help with the spectropolarimetric observations. P.D. acknowledges the financial support of NSERC. This work was also supported by the NSF through grant AST 03-07321. Support from the Reardon Foundation is also gratefully acknowledged.

REFERENCES

- Beauchamp, A. 1995, Ph.D. Thesis, Université de Montréal
- Beauchamp, A., Wesemael, F., & Bergeron, P. 1997, *ApJS*, 108, 559
- Bergeron, P., Saumon, D., & Wesemael, F. 1995, *ApJ*, 443, 764
- Behara, N., & Jeffery, C. S. 2005, in *ASP Conf. Ser. 334*, 14th European Workshop on White Dwarfs, ed. D. Koester & S. Moehler (San Francisco: ASP), 253
- Behara, N. T., & Jeffery, C. S. 2006, *A&A*, 451, 643
- Brassard, P., Fontaine, G., Dufour, P., & Bergeron, P. 2007, in *ASP Conf. Ser. 372*, 15th European Workshop on White Dwarfs, ed. R. Napiwotzki & M. R. Burleigh (San Francisco: ASP), 19
- D’Antona, F., & Mazzitelli, I. 1987, *IAU Colloq. 95: Second Conference on Faint Blue Stars*, 635
- Desharnais, S., Wesemael, F., Chayer, P., Kruk, J. W., & Saffer, R. A. 2008, *ApJ*, 672, 540
- Dufour, P., Wesemael, F., & Bergeron, P. 2002, *ApJ*, 575, 1025
- Dufour, P., Bergeron, P., & Fontaine, G. 2005, *ApJ*, 627, 404
- Dufour, P., Bergeron, P., Schmidt, G. D., Liebert, J., Harris, H. C., Knapp, G. R., Anderson, S. F., & Schneider, D. P. 2006, *ApJ*, 651, 1112
- Dufour, P., Liebert, J., Fontaine, G., & Behara, N. 2007a, *Nature*, 450, 522
- Dufour, P., et al. 2007b, *ApJ*, 663, 1291

- Dufour, P. 2007c, Ph.D. Thesis, Université de Montréal
- Dufour, P., Liebert, J., Fontaine, G., & Behara, N. 2007d, ArXiv e-prints, 711
- Eisenstein, D. J., et al. 2006, *ApJS*, 167, 40
- Fontaine, G., & van Horn, H. M. 1976, *ApJS*, 31, 467
- Fontaine, G., & Brassard, P. 2005, in ASP Conf. Ser. 334, 14th European Workshop on White Dwarfs, ed. D. Koester & S. Moehler (San Francisco: ASP), 49
- Fontaine, G., Brassard, P., & Dufour, P. 2008, ArXiv e-prints, 803
- Fukugita, M., Ichikawa, T., Gunn, J. E., Doi, M., Shimasaku, K., & Schneider, D. P. 1996, *AJ*, 111, 1748
- García-Berro, E., & Iben, I., Jr. 1994, *ApJ*, 434, 306
- García-Berro, E., Ritossa, C., & Iben, I., Jr. 1997, *ApJ*, 485, 765
- Herwig, F., Blöcker, T., Langer, N., & Driebe, T. 1999, *A&A*, 349, L5
- Hogg, D. W., Finkbeiner, D. P., Schlegel, D.J., & Gunn, J. E., 2001, *AJ*, 122, 2129
- Hubeny, I. 1988, *Computer Physics Communications*, 52, 103
- Hummer, D. G., & Mihalas, D. 1988, *ApJ*, 331, 794
- Iben, I., Jr. 1984, *ApJ*, 277, 333
- Iben, I., Jr., Ritossa, C., & García-Berro, E. 1997, *ApJ*, 489, 772
- Ivezić, Z., et al. 2004, *Astron. Nachr.*, 325, 583
- Kalirai, J. S., Bergeron, P., Hansen, B. M. S., Kelson, D. D., Reitzel, D. B., Rich, R. M., & Richer, H. B. 2007, *ApJ*, 671, 748
- Kawai, Y., Saio, H., & Nomoto, K. 1988, *ApJ*, 328, 207
- Koester, D., & Schönberner, D. 1986, *A&A*, 154, 125
- Koester, D., & Knist, S. 2006, *A&A*, 454, 951
- Kurucz, R. L., & Avrett, E. H. 1981, *SAO Special Report*, 391, 1
- Liebert, J., et al. 2003, *AJ*, 126, 2521

- McCook, G. P., & Sion, E. M. 1999, *ApJS*, 121, 1
- Montgomery, M. H., Williams, K. A., Winget, D. E., Dufour, P., DeGennaro, S., & Liebert, J. 2008, *ArXiv e-prints*, 803
- Nousek, J. A., Shipman, H. L., Holberg, J. B., Liebert, J., Pravdo, S. H., White, N. E., & Giommi, P. 1986, *ApJ*, 309, 230
- Peach, G. 1970, *MmRAS*, 73, 1
- Pelletier, C., Fontaine, G., Wesemael, F., Michaud, G., & Wegner, G. 1986, *ApJ*, 307, 242
- Petitclerc, N., Wesemael, F., Kruk, J. W., Chayer, P., & Billères, M. 2005, *ApJ*, 624, 317
- Press, W. H., Teukolsky, S. A., Vetterling, W. T., & Flannery, B. P. 1992, *Numerical Recipes in FORTRAN*, 2nd edition (Cambridge: Cambridge University Press), 644
- Provencal, J. L., Shipman, H. L., Thejll, P., & Vennes, S. 2000, *ApJ*, 542, 1041
- Provencal, J. L., Shipman, H. L., Koester, D., Wesemael, F., & Bergeron, P. 2002, *ApJ*, 568, 324
- Ritossa, C., García-Berro, E., & Iben, I., Jr. 1996, *ApJ*, 460, 489
- Ritossa, C., García-Berro, E., & Iben, I., Jr. 1999, *ApJ*, 515, 381
- Schlegel, D. J., Finkbeiner, D. P., & Davis, M. 1998, *ApJ*, 500, 525
- Schmidt, G. D., Stockman, H. S., & Smith, P. S. 1992, *ApJ*, 398, L57
- Smith, J. A., et al. 2002, *AJ*, 123, 2121
- Thejll, P., Shipman, H. L., MacDonald, J., & Macfarland, W. M. 1990, *ApJ*, 361, 197
- The Opacity Project Team 1995, *The Opacity Project*, Vol. 1, Institute of Physics, Bristol
- The Opacity Project Team 1997, *The Opacity Project*, Vol. 2, Institute of Physics, Bristol
- Voss, B., Koester, D., Napiwotzki, R., Christlieb, N., & Reimers, D. 2007, *A&A*, 470, 1079
- Wegner, G., & Koester, D. 1985, *ApJ*, 288, 746
- Werner, K. 1991, *A&A*, 251, 147
- Werner, K., & Wolff, B. 1999, *A&A*, 347, L9

Werner, K., Rauch, T., Barstow, M. A., & Kruk, J. W. 2004, *A&A*, 421, 1169

Werner, K., & Herwig, F. 2006, *PASP*, 118, 183

Table 1. Atmospheric Parameters of Hot DQ Stars from the SDSS

Name	plate	MJD	Fiber	$T_{\text{eff}}(\text{K})$	$\log g$	$\log C/\text{H}$	$\log C/\text{He}$	D (pc)
SDSS J000555.90–100213.3	650	52143	37	19420 (920)	8.0	-	-	255
SDSS J010647.92+151327.8	422	51878	422	23430 (1680)	8.0	-	1.00	492
SDSS J023637.42–073429.5	455	51909	403	21110 (430)	8.0	-	-	738
SDSS J115305.54+005646.2	284	51943	533	21650 (320)	8.0	-	-	515
SDSS J133710.19+002643.7	299	51671	305	21670 (245)	8.0	1.67	-	461
SDSS J142625.70+575218.4	789	52342	197	19830 (750)	9.0	-	0.0	245
SDSS J161531.71+454322.4	814	52443	577	20940 (460)	8.0	1.74	-	719
SDSS J220029.09–074121.5	717	52468	462	21240 (180)	8.0	-	-	283
SDSS J234843.30–094245.2	648	52559	585	21550 (340)	8.0	-	-	544

Fig. 1.— Representative synthetic spectra of Hot DQ white dwarfs taken from our model grid for various effective temperatures, gravities, helium and hydrogen abundances. The spectra are normalized to unity at 4200 Å and offset by an arbitrary factor for clarity. The labels indicate the effective temperature, while the color of each spectrum corresponds to a different gravity, as indicated in the lower left corner. The bottom two examples show the influence of trace helium ($\log(C/\text{He}) = 2, 1$ and 0) and trace hydrogen ($\log(C/\text{H}) = 2, 1$ and 0) while in blue, we show the $\log g = 8$ synthetic spectra for pure helium atmosphere (DB) and pure hydrogen atmosphere (DA).

Fig. 2.— Observed circular polarization (top panel) and the corresponding spectrum obtained with a spectral resolution ($\Delta\lambda \sim 17$ Å). The thick marks indicate the position of the strongest C II features.

Fig. 3.— Fits to the energy distribution (right panel) and carbon lines (left panel) for all carbon dominated DQ white dwarfs in our SDSS sample. The *ugriz* photometric observations are represented by error bars, while the average model fluxes are shown by filled circles. The derived atmospheric parameters are indicated in each panel. We have applied for clarity a three-point average window smoothing in the display of the spectroscopic data.

Fig. 4.— Comparison of a pure helium DB model (red line) with a pure carbon model (blue line) for $\log g = 8.0$ and $T_{\text{eff}} = 22,000$ K. Note that $\int H_{\nu} d\nu$ is the same for both models ($= \sigma T_{\text{eff}}^4 / 4\pi$).

Fig. 5.— Comparison of the optical spectra of pure composition atmospheres composed of hydrogen, helium, carbon and oxygen for $\log g = 8.0$ and $T_{\text{eff}} = 22,000$ K.

Fig. 6.— Comparison of synthetic spectra of a pure carbon atmosphere models (blue) with a $\log(C/\text{He}) = -3.0$ model (red) for $T_{\text{eff}} = 10,000$ K and $\log g = 8.0$. Spectra with extremely strong carbon bands similar to that predicted in the pure carbon model should have been easily noticed in SDSS if they existed.

Fig. 7.— Schematic representation of our proposed evolutionary scenario to explain the existence of carbon dominated atmosphere white dwarfs.

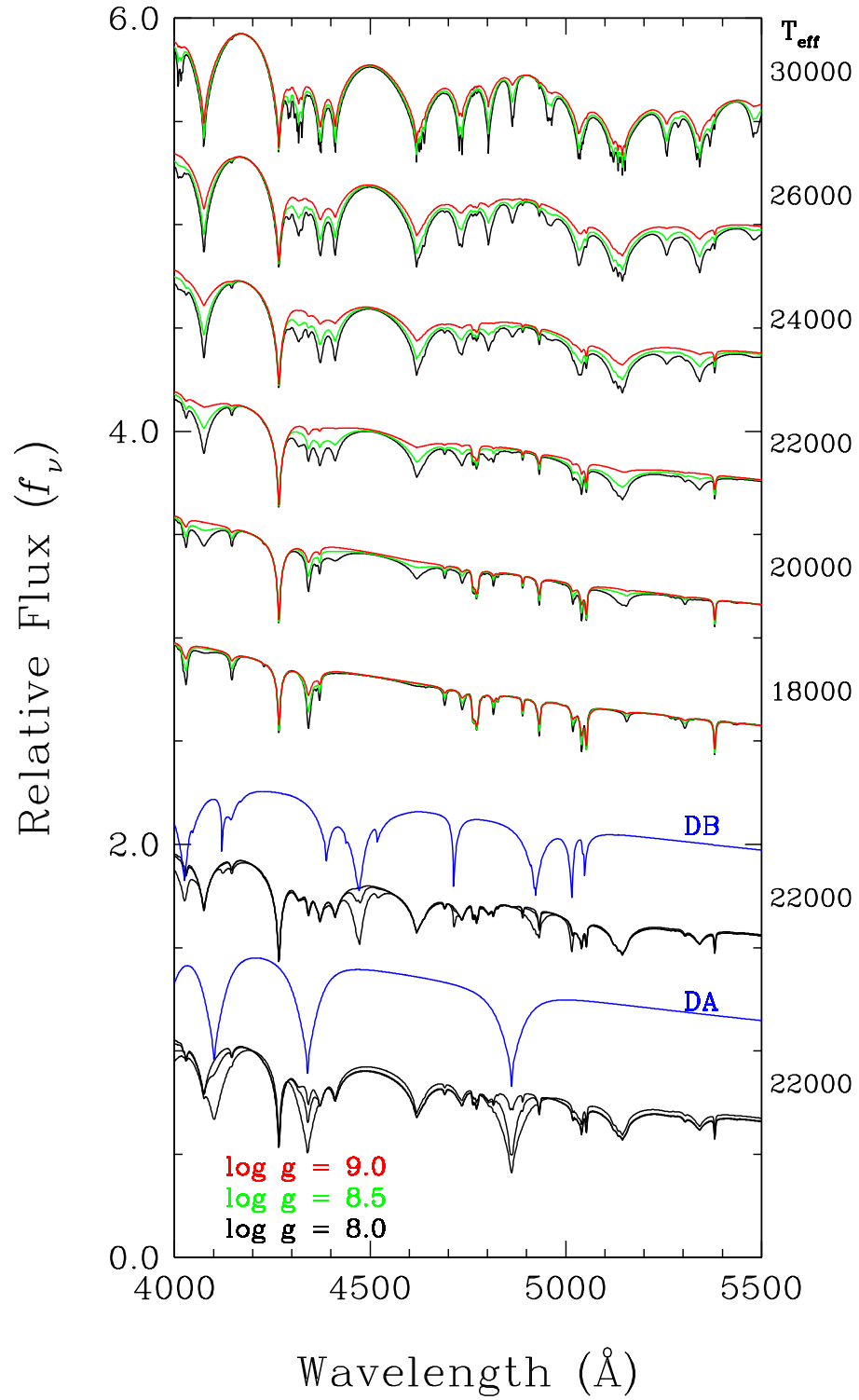
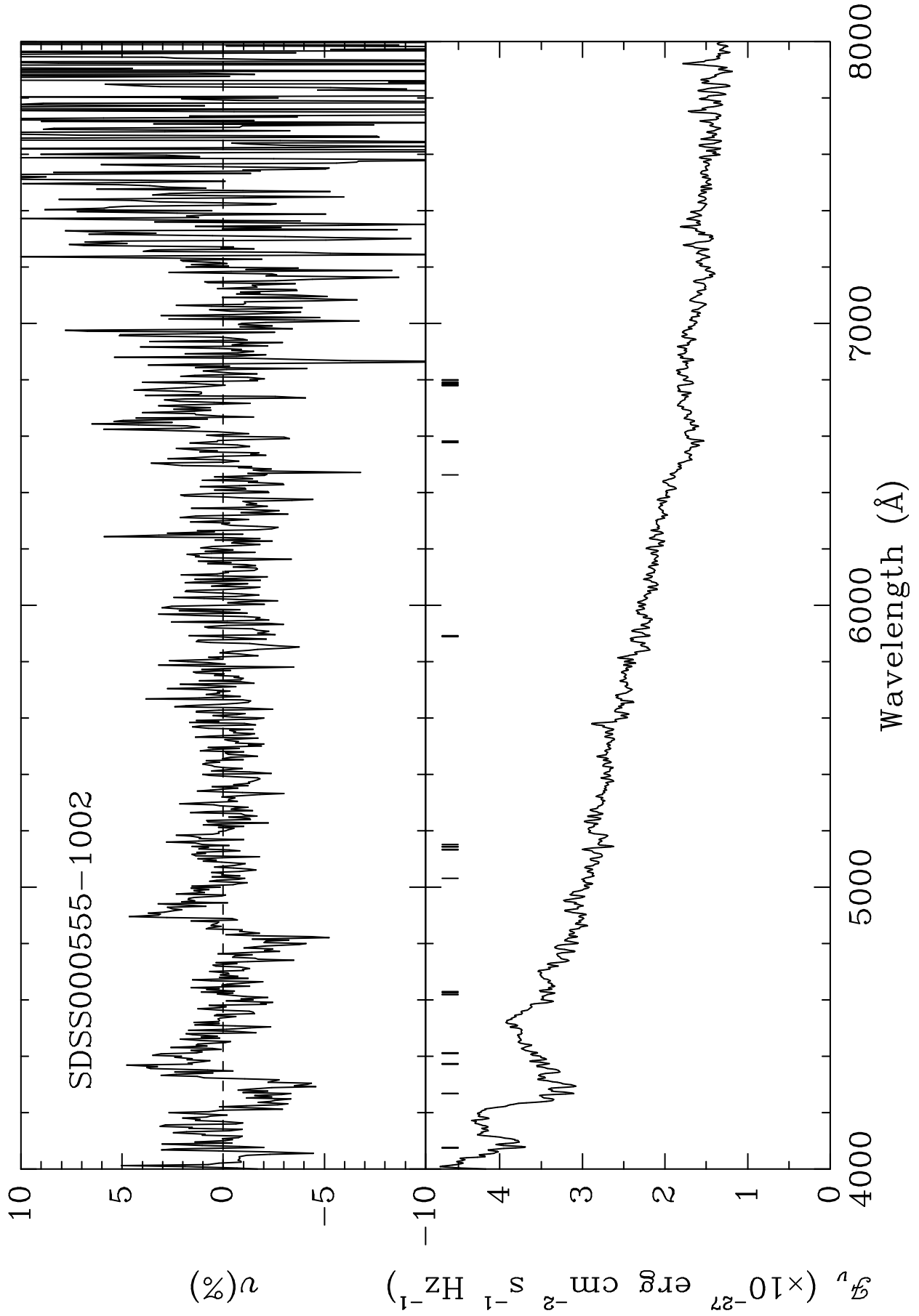


Figure 1



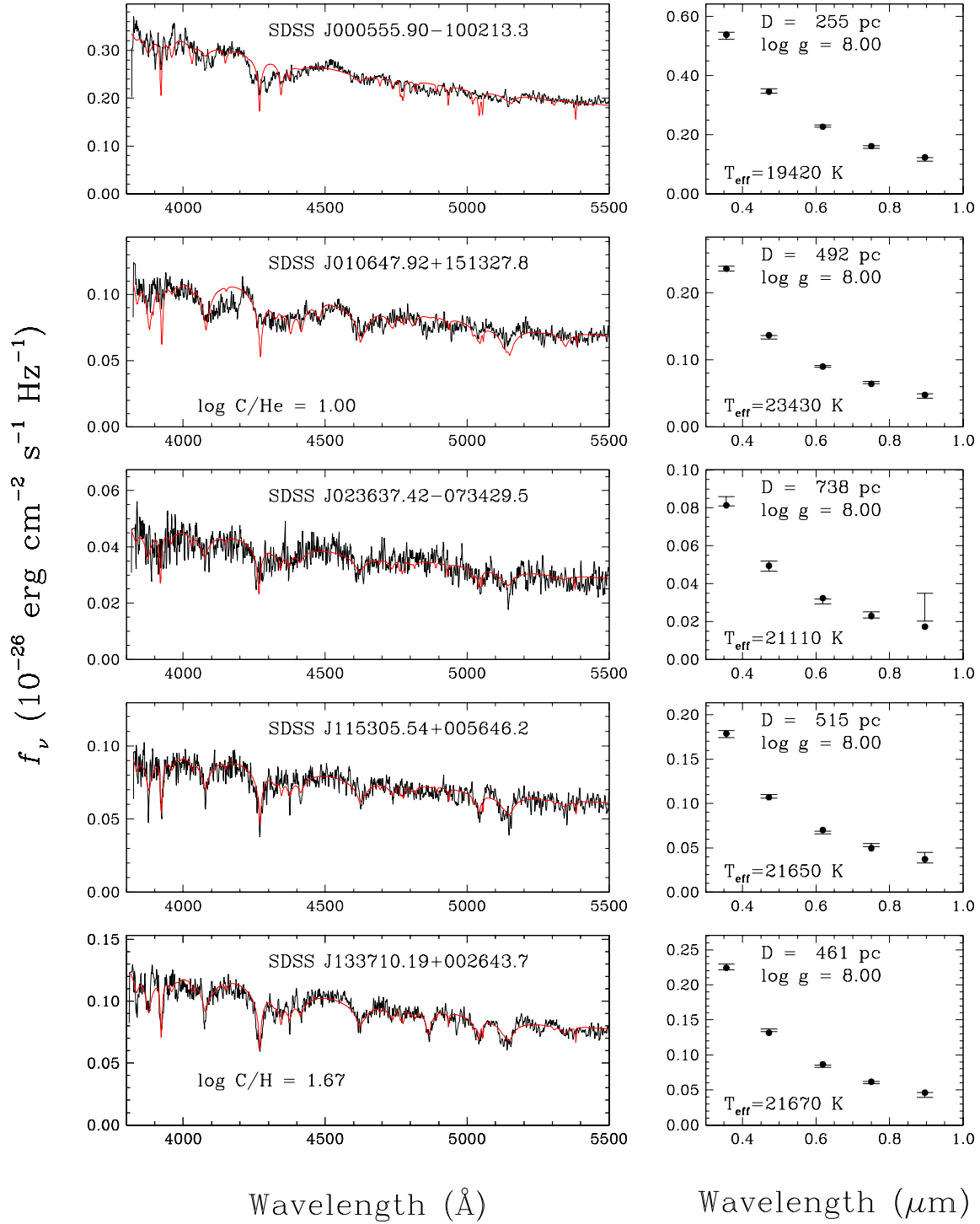


Figure 3

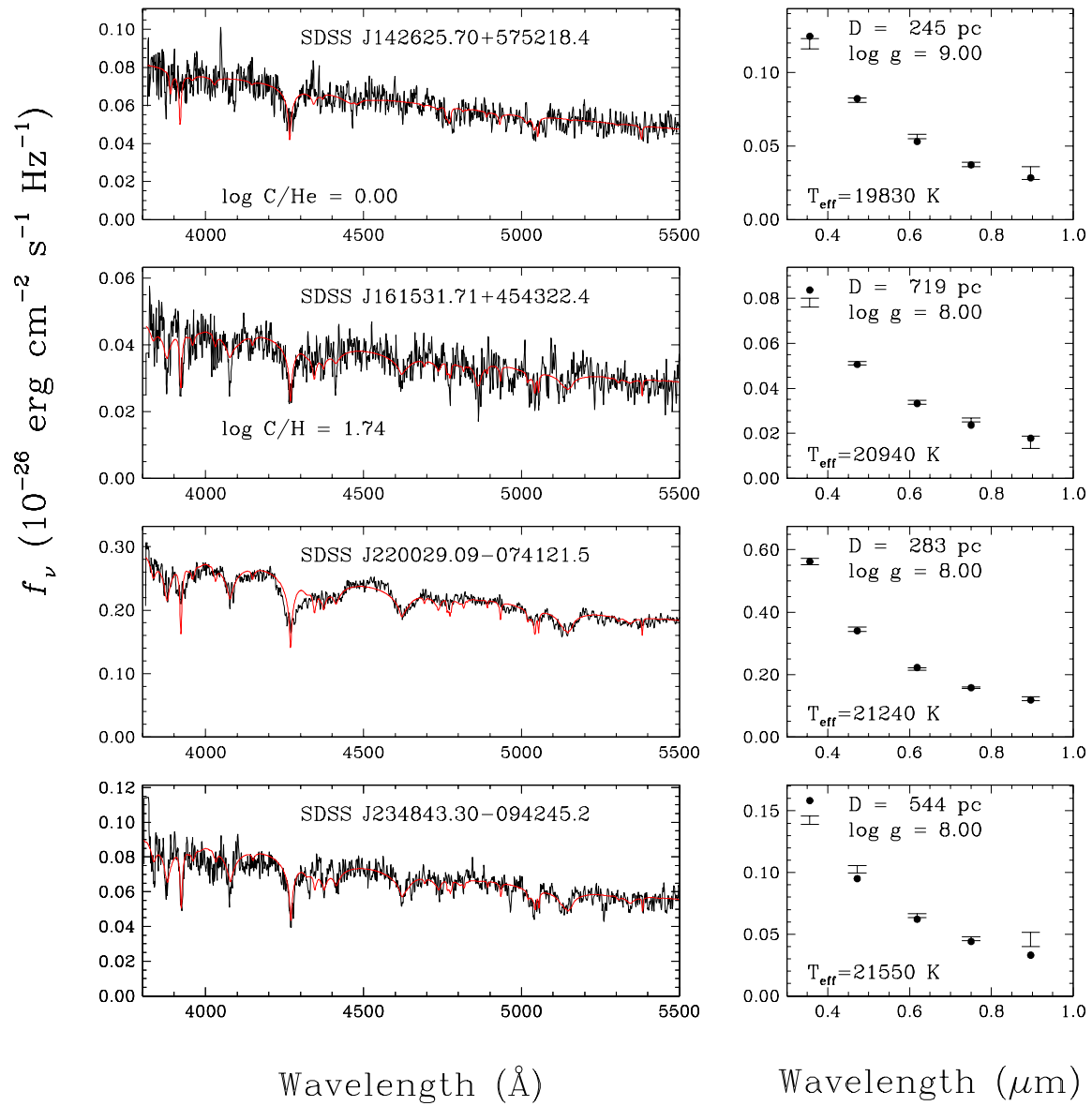


Figure 3

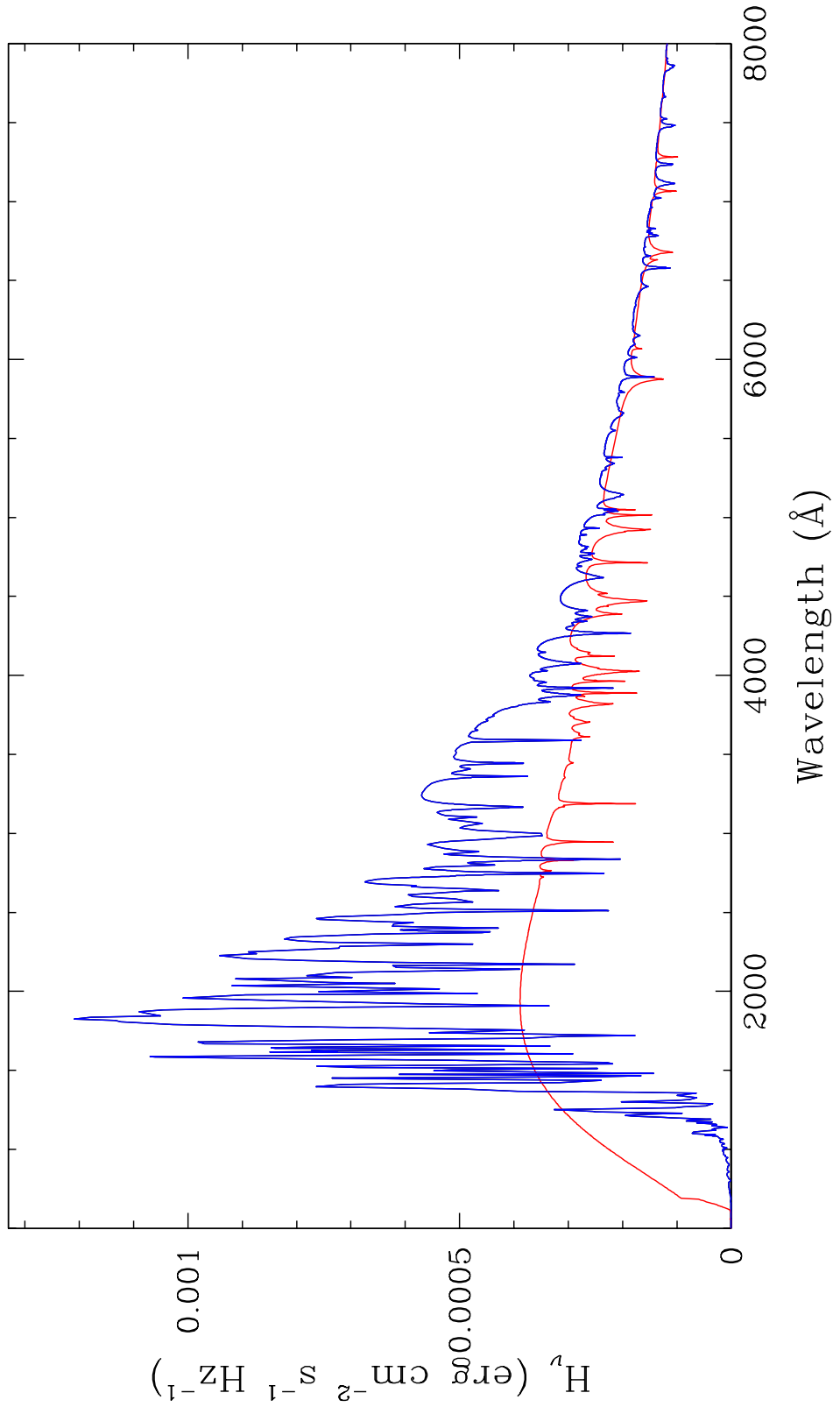


Figure 4

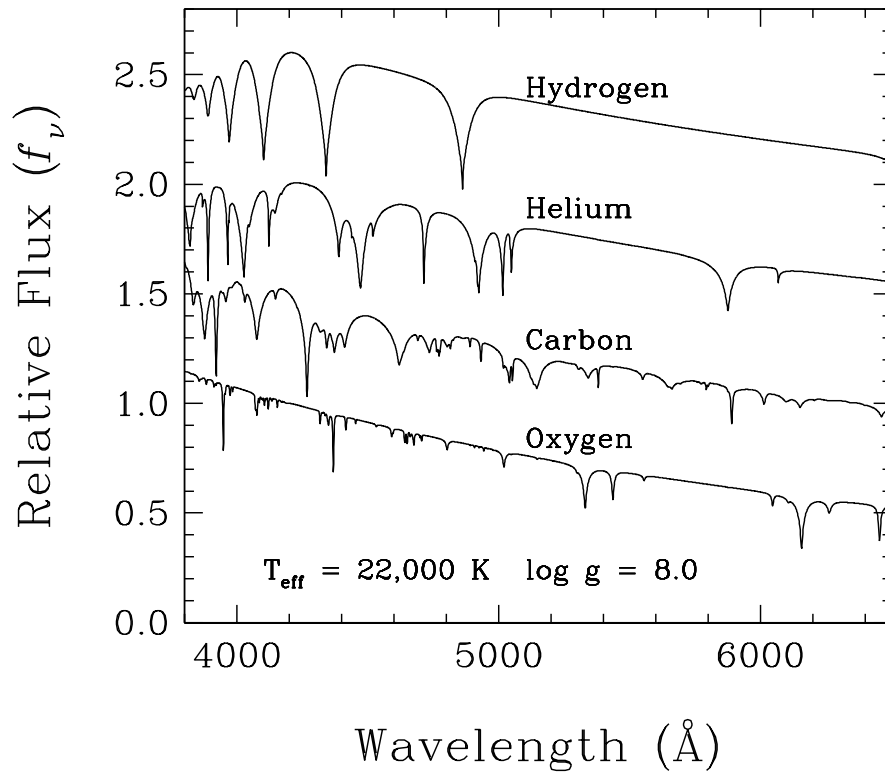


Figure 5

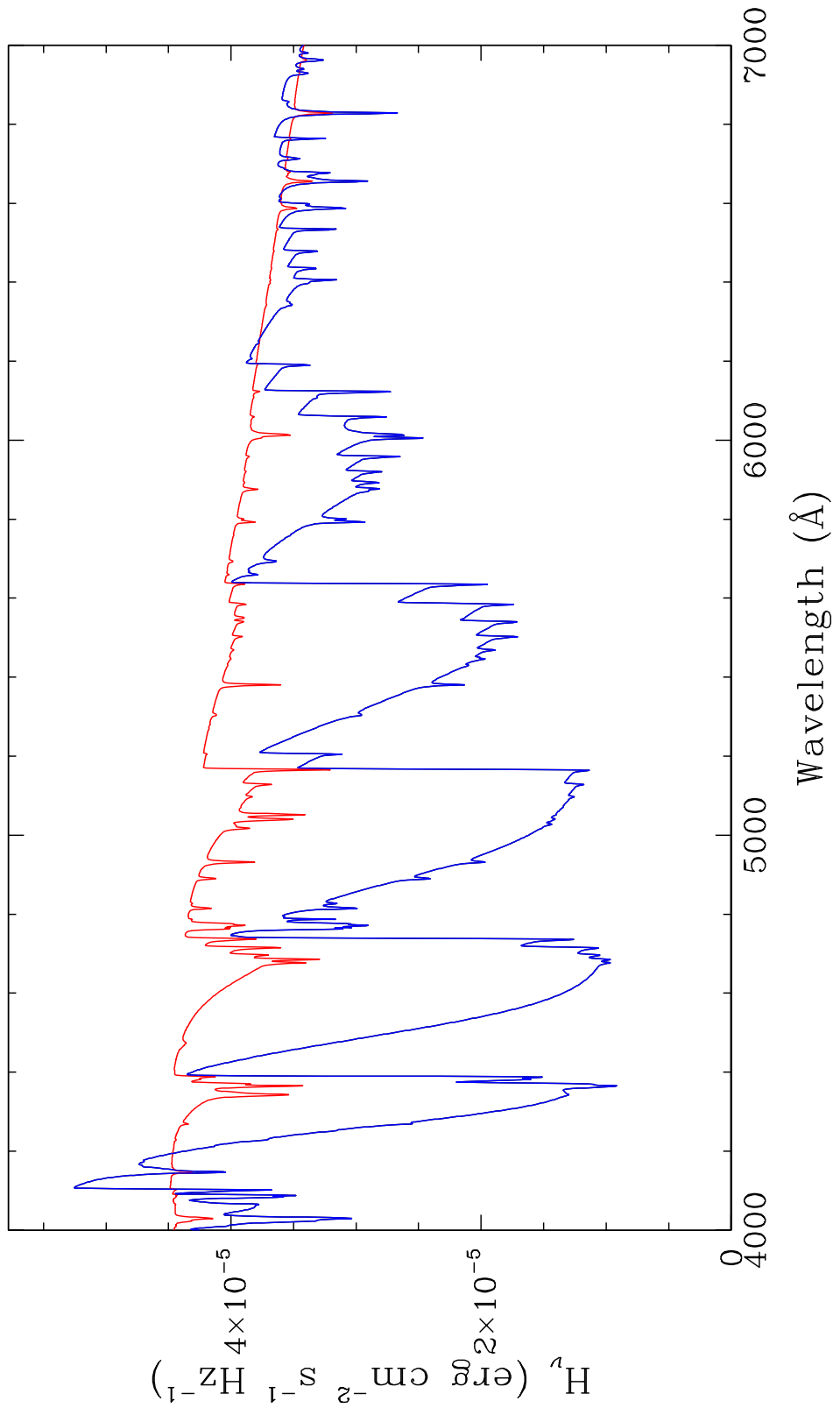


Figure 6

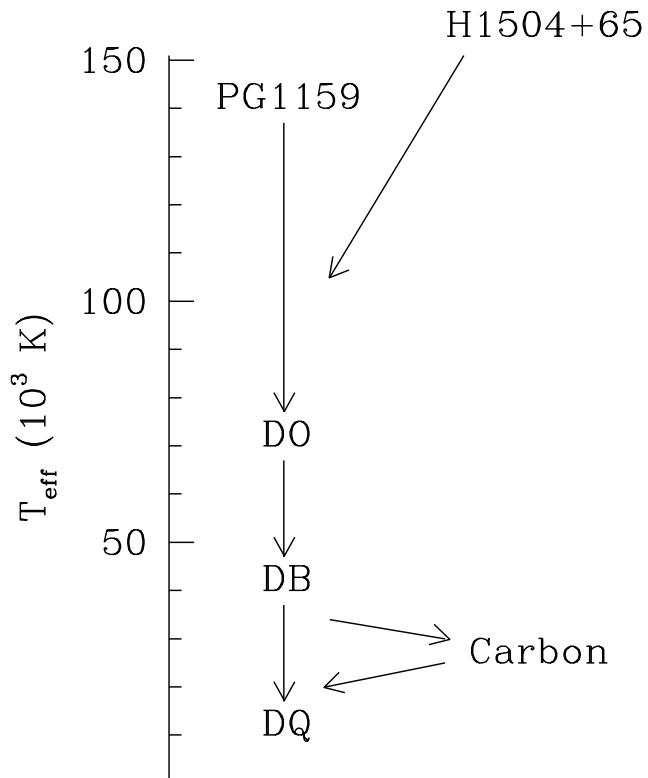


Figure 7